Mitigating parametric instabilities in plasmas by sunlight-like lasers EP

H. H. Ma, X. F. Li, S. M. Weng, et al.

COLLECTIONS

EP   This paper was selected as an Editor's Pick

View Online   Export Citation   CrossMark

Matter and
Radiation at Extremes

Special Issue: High Pressure Science

READ NOW!

Mitigating parametric instabilities in plasmas by sunlight-like lasers ᴱᴾ

H. H. Ma,[1,2,3] X. F. Li,[1,2,4,a)] S. M. Weng,[1,2,a)] S. H. Yew,[1,2] S. Kawata,[3] P. Gibbon,[4,5]
Z. M. Sheng,[1,2,6,7,a)] and J. Zhang[1,2]

AFFILIATIONS

[1] Key Laboratory for Laser Plasmas (MoE), School of Physics and Astronomy, Shanghai Jiao Tong University, Shanghai 200240, China
[2] Collaborative Innovation Center of IFSA, Shanghai Jiao Tong University, Shanghai 200240, China
[3] Graduate School of Engineering, Utsunomiya University, Yohtoh 7-1-2, Utsunomiya 321-8585, Japan
[4] Institute for Advanced Simulation, Jülich Supercomputing Centre, Forschungszentrum Jülich, 52425 Jülich, Germany
[5] Centre for Mathematical Plasma Astrophysics, Katholieke Universiteit Leuven, 3000 Leuven, Belgium
[6] SUPA, Department of Physics, University of Strathclyde, Glasgow G4 0NG, United Kingdom
[7] Tsung-Dao Lee Institute, Shanghai Jiao Tong University, Shanghai 200240, China

[a)] Authors to whom correspondence should be addressed: xiaofengli@sjtu.edu.cn; wengsuming@sjtu.edu.cn;
and z.sheng@strath.ac.uk

ABSTRACT

Sunlight-like lasers that have a continuous broad frequency spectrum, random phase spectrum, and random polarization are formulated theoretically. With a sunlight-like laser beam consisting of a sequence of temporal speckles, the resonant three-wave coupling that underlies parametric instabilities in laser–plasma interactions can be greatly degraded owing to the limited duration of each speckle and the frequency shift between two adjacent speckles. The wave coupling can be further weakened by the random polarization of such beams. Numerical simulations demonstrate that the intensity threshold of stimulated Raman scattering in homogeneous plasmas can be doubled by using a sunlight-like laser beam with a relative bandwidth of ~1% as compared with a monochromatic laser beam. Consequently, the hot-electron generation harmful to inertial confinement fusion can be effectively controlled by using sunlight-like laser drivers. Such drivers may be realized in the next generation of broadband lasers by combining two or more broadband beams with independent phase spectra or by applying polarization smoothing to a single broadband beam.

I. INTRODUCTION

As one of the most critical and fundamental problems that arise in attempts to achieve inertial confinement fusion (ICF), parametric instabilities have attracted significant attention for many years.[1,2] With the construction of high-power lasers at higher energy for either direct- or indirect-drive approaches to ICF,[3,4] it becomes more urgent to control parametric instabilities in laser–plasma interactions.[5,6] In the indirect-drive approach, for example, laser beams have to propagate through a large-scale relatively uniform underdense plasma before arriving at the hohlraum wall and converting their energy into soft x rays that drive the final implosion of the fusion capsule.[7,8] The parametric instabilities involved here include for

example, stimulated Raman scattering (SRS),[9,10] stimulated Brillouin scattering (SBS),[11] and cross-beam energy transfer (CBET).[12,13] These parametric instabilities not only scatter away a considerable proportion of the laser energy, but may also produce harmful hot electrons that affect compression and implosion efficiency.[5,6,14,15]

So far, a number of strategies have been employed or proposed for mitigating parametric instabilities. Above all, the commonly used frequency-tripled lasers significantly reduce parametric instabilities. since the growth rates of these instabilities usually increase with the laser wavelength.[7] Beam smoothing schemes such as spectral dispersion (SSD),[16] continuous phase plates (CPPs),[17] and polarization smoothing (PS)[18] have been widely used to control the peak

intensities of laser spatial speckles and hence to suppress instabilities.[19–22] In multi-ion-species plasmas[11] or highly magnetized plasmas,[23] parametric instabilities may be reduced by enhanced Landau damping. By using laser pulses with spike trains of uneven duration and delay (STUD),[24] the development of parametric instability can be periodically suspended and damped. The use of laser beams with rotating polarizations has been proposed as a method to suppress parametric instabilities by weakening the three-wave coupling between incident light, scattered light, and stimulated plasma waves.[25]

More generally, parametric instabilities would be suppressed if the three-wave coupling were broken, which could be realized by using broadband lasers. Theoretical analyses and simulations have long predicted that parametric instabilities can be significantly suppressed if the laser bandwidth is larger than the instability growth rates.[26–28] With innovations in the generation of high-energy broadband laser pulses,[29–31] more effort is now being devoted to the suppression of parametric instabilities by broadband lasers. Theoretical and experimental studies have shown that broadband lasers can increase the intensity thresholds for parametric instabilities and reduce the corresponding reflections.[32–37] Nevertheless, the bandwidths required to adequately suppress parametric instabilities (especially SRS) are usually too large and beyond the capabilities of contemporary high-power laser technology. Reduction of the bandwidth requirement for suppressing parametric instabilities is therefore of particular interest for ICF experiments.

In this paper, we propose a novel scheme for mitigating parametric instabilities using a sunlight-like laser, which can dramatically raise the intensity thresholds for instabilities with a much smaller bandwidth in comparison with conventional broadband lasers. For the first time, we formulate the temporal electric field structure of a sunlight-like laser that has a continuous broad spectrum, random phase, and random polarization. It is found that a sunlight-like laser pulse consists of a sequence of speckles with different durations and central frequencies. With an increase in the sunlight-like laser bandwidth, the mean shift between the central frequencies of two adjacent speckles increases. Consequently, the resonant three-wave coupling for parametric instabilities within one speckle may no longer be supported in the next speckle. More importantly, the random polarization further decreases the growth rates of parametric instabilities. Therefore, sunlight-like laser pulses have obvious superiority in mitigating parametric instabilities in comparison with conventional broadband lasers. As an example, the efficient mitigation of SRS with sunlight-like laser pulses has been demonstrated by numerical simulations. In this study, we focus on the mitigation of SRS, since this type of instability usually has a higher growth rate, and its mitigation requires a larger bandwidth and is more challenging than other instabilities.

II. SPECIFIC MODELS FOR BROADBAND LASERS AND SUNLIGHT-LIKE LASERS

In previous studies, a broadband laser beam has usually been modeled as a superposition of many monochromatic laser beams that have random phases and different carrier frequencies within a given bandwidth.[26,28,33,34,36,37] Although this method is convenient for implementation in numerical simulation codes, the frequency spectrum of the resulting broadband laser beam will deviate from the

initially assumed spectrum if the number of monochromatic laser beams is chosen arbitrarily (see the supplementary material). As a necessary preliminary to the study of the suppression of parametric instabilities by broadband lasers, the electric field of a broadband laser light should be modeled precisely. Here, we propose a natural way to model the electric fields of broadband lasers with continuous frequency spectra as observed in experiments.

First, the amplitude frequency spectrum of a broadband laser light is assumed to be $f(\omega)$. This is then converted to a complex field by considering the random phase of the broadband laser, i.e.,

$$F(\omega) = f(\omega)\exp[i\phi(\omega)], \tag{1}$$

where the amplitude-phase frequency spectrum $F(\omega)$ is introduced, the phase frequency spectrum $\phi(\omega)$ changing within $0 < \phi < 2\pi$ is a random function of the frequency ω, and i is the imaginary unit. The electric field $E(t)$ of a broadband laser in the time domain can then be obtained by the following inverse Fourier transform of the amplitude-phase frequency spectrum

$$E(t) = \mathcal{F}^{-1}[F(\omega)], \tag{2}$$

where $\mathcal{F}^{-1}$ denotes the inverse Fourier transform. According to Eq. (1), the amplitude-phase frequency spectrum $F(\omega)$ changes with different random phase spectra. Consequently, the electric fields $E(t)$ of two broadband lasers with the same amplitude frequency spectrum can be completely different if their phase frequency spectra are different. Therefore, if two independent broadband laser beams (with
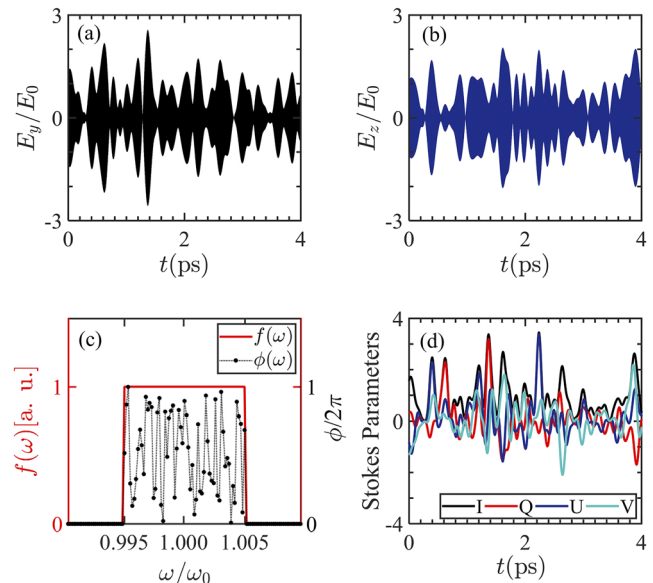

FIG. 1. Properties of a sunlight-like laser pulse with a flat-top frequency spectrum and bandwidth $\Delta\omega/\omega_0 = 1\%$. The sunlight-like laser is modeled by Eqs. (1)–(3), where the central frequency $\omega_0 = 2\pi c/\lambda$ with $\lambda = 351$ nm. (a) and (b) Electric field components E_y and E_z, respectively, where the time-averaged electric field amplitude $E_0 = \sqrt{\langle E_y^2(t)\rangle} = \sqrt{\langle E_z^2(t)\rangle}$. (c) Amplitude frequency spectrum $f(\omega)$ and phase frequency spectrum $\phi(\omega)$ of E_y. (d) Stokes parameters of the sunlight-like laser pulse, where I denotes the intensity regardless of polarization, Q the linear polarization along the y (+) or z (−) axis, U the linear polarization at + 45° (+) or −45° (−) from the y axis, and V the right-handed (+) or left-handed (−) circular polarization.[38]

two different random phase frequency spectra) are set with mutually orthogonal polarizations, one can obtain a kind of sunlight-like laser beam that has a continuous broad frequency spectrum, random phase spectrum, and random polarization. The electric field of a sunlight-like laser can thus be written as

$$\mathbf{E}(t) = E_y(t)\mathbf{e}_y + E_z(t)\mathbf{e}_z, \quad (3)$$

where the light is assumed to propagate along the x axis, and E_y and E_z are the electric fields along two orthogonal polarization directions that are modeled by using Eq. (2) twice independently.

As an example, the electric fields E_y and E_z obtained from the above model for a sunlight-like laser pulse with a flat-top frequency spectrum and bandwidth $\Delta\omega/\omega_0 = 1\%$ are displayed in Figs. 1(a) and 1(b), respectively. Although these electric fields appear to be temporally irregular, their Fourier transforms perfectly reproduce the assumed flat-top frequency spectrum and random phase spectrum. The Fourier transform results of E_y are illustrated in Fig. 1(c), while the Fourier transform of E_z reproduces the same amplitude spectrum $f(\omega)$ but a different random phase spectrum $\phi(\omega)$. Besides the flat-top frequency spectrum, the model can reproduce any assumed frequency spectrum, such as a Gaussian spectrum (see the supplementary material). Further, the random polarization of a sunlight-like laser is evidenced by the chaotically oscillating Stokes parameters, as shown in Fig. 1(d). The random polarization of a sunlight-like laser is also visualized in the movie in the supplementary material. To some extent, the light from a sunlight-like laser as given by Eq. (3) can be

considered as broadband elliptically polarized light whose polarization orientation, axial ratio, and handedness change randomly with time. The above analysis indicates that Eqs. (1)–(3) can precisely model a sunlight-like laser pulse with a continuous spectrum, random phase, and random polarization.

It is worth noting that the electric field envelope in Fig. 1(a) consists of a sequence of temporal speckles that have different peak amplitudes and durations. Two typical adjacent speckles are displayed in detail in Fig. 2(a), where the speckle duration is defined as the time interval between two adjacent valleys in the envelope. More importantly, the Fourier transforms of these two speckle electric fields result in two different frequency spectra, where a shift $\delta\omega$ between their central frequencies is clearly evidenced in Fig. 2(b).

To quantify the effect of laser bandwidth on the mean frequency shift between adjacent speckles and the mean speckle duration, a series of statistical analyses are carried out using 100 independent broadband laser lights for each bandwidth. In these statistical analyses, the effect of spectral resolution is also investigated by using three different total pulse durations (7.02, 14.04, and 21.06 ps); the relation between the spectral resolution and the laser pulse duration can be found in the supplementary material. As shown in Figs. 2(c) and 2(d), the statistical analyses reveal that the mean central frequency shift between adjacent speckles is proportional to the bandwidth ($\langle\delta\omega\rangle \simeq 0.16\Delta\omega$), while the mean speckle duration is inversely proportional to the bandwidth ($\langle\delta t\rangle \simeq 9.4/\Delta\omega$). Figures 2(c) and 2(d) also indicate that the statistical characters of the speckles are independent of the numerical spectral resolution used in the statistics, which illustrates that both the mean frequency shift between two adjacent speckles and the mean speckle duration are intrinsic physical properties of a broadband laser light.

The intrinsic properties of sunlight-like lasers suggest that they can mitigate parametric instabilities in three key ways. First, the entire laser pulse is divided into many speckles, with each speckle having only a short duration, which limits the interaction time between each speckle and the plasma. Second, owing to the frequency shift between adjacent speckles, the three-wave coupling within one speckle is not fully inherited by the next speckle, which suggests that the plasma waves excited by the first speckle may not be continuously amplified by the next. Third, the random polarization greatly reduces the growth rates of instabilities, since the three-wave coupling essentially breaks if the polarization directions of the rear incident light and the front scattered light are orthogonal. The first two mechanisms may work only if the bandwidth is large enough, but they become more and more important with increasing bandwidth, since $\langle\delta t\rangle \propto 1/\Delta\omega$ and $\langle\delta\omega\rangle \propto \Delta\omega$. The third mechanism, however, can play a significant role even with a moderate bandwidth. In the present experiments, the maximum achievable relative bandwidth of the broadband laser is only about 1%. Therefore, it becomes more necessary to use sunlight-like lasers in the mitigation of parametric instabilities, by taking advantage of their random polarizations.

FIG. 2. Properties of temporal speckles in a sunlight-like laser pulse. (a) Electric fields of two typical adjacent speckles (denoted by "S1" and "S2") corresponding to E_y within 0.3–0.7 ps in Fig. 1(a). (b) Amplitude spectra $f_{S1}(\omega)$ and $f_{S2}(\omega)$ of these two speckles, showing the obvious frequency shift $\delta\omega$ between them. (c) Statistical mean frequency shift $\langle\delta\omega\rangle$ between the central frequencies of two adjacent speckles as a function of bandwidth. (d) Statistical mean duration $\langle\delta t\rangle$ of a single speckle as a function of bandwidth. The statistical analyses in (c) and (d) are performed over all adjacent speckles for $\langle\delta\omega\rangle$ and over all speckles for $\langle\delta t\rangle$, with 100 independent broadband laser beams for each bandwidth. The statistical results under different spectral resolutions are compared by using three different laser pulse durations: $6000T_0$ (7.02 ps), $12\,000T_0$ (14.04 ps), and $18\,000T_0$ (21.06 ps).

III. PIC SIMULATIONS OF THE SUPPRESSION OF PARAMETRIC INSTABILITIES BY SUNLIGHT-LIKE LASERS

To verify the superiority of sunlight-like laser drivers in mitigating parametric instabilities, a series of 1D and 2D particle-in-cell (PIC) simulations are performed using the EPOCH code.[39] Both 1D
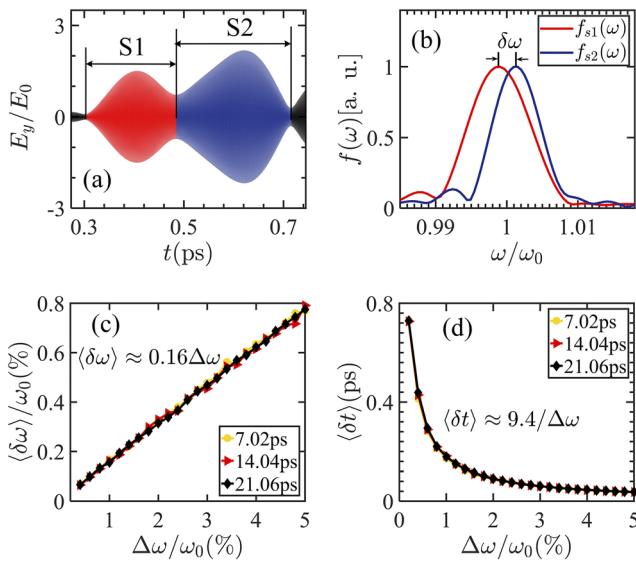
and 2D EPOCH codes are first modified to input the electric fields of broadband lasers and sunlight-like lasers according to Eqs. (1)–(3). In the simulations, the plasma has a uniform density $n_e = 0.128 n_c$ and an electron temperature of 3 keV, where n_c is the critical density corresponding to an incident laser wavelength $\lambda = 351$ nm. The ions are assumed to be immobile. In the 1D simulations, the simulation box has a total length of 150λ, and the homogeneous plasma slab occupies the region $30\lambda < x < 130\lambda$. The plasma slab also has a 5λ density slope at each side. The cell size is $\Delta x = 0.01\lambda$, with 600 macroparticles per cell. An open boundary condition is set for each side of the simulation box. In the 2D simulations, the plasma occupies the region $5\lambda < x < 105\lambda$ and $0 < y < 40\lambda$. The cell size is $\Delta x = \Delta y = 0.02\lambda$, with 100 macroparticles per cell. A periodic boundary condition is adopted in the y direction and an open boundary condition in the x direction. The simulations run up to $6000\lambda/c \simeq 7$ ps for 1D and $1500\lambda/c \simeq 1.75$ ps for 2D cases. To compare the effects of different laser types in suppressing SRS, the simulations are carried out using monochromatic lasers, broadband lasers, and sunlight-like lasers.

In Fig. 3(a), the SRS reflectivity R_{SRS} within a certain laser intensity range relevant to ICF research is compared for monochromatic lasers, broadband lasers, and sunlight-like lasers. Here, the SBS reflectivity is excluded by using immobile ions. In analogy with previous studies,[40,41] we find that in each case R_{SRS} rises steeply around an intensity threshold and then converges slowly to a saturation value with increasing laser intensity. Here we define the SRS threshold as the intensity at which $R_{SRS} = 1\%$, since the slope of the rising reflectivity has its maximum at around $R_{SRS} \simeq 1\%$, as shown in Fig. 3(a). By comparison with the monochromatic laser, the SRS intensity threshold for the broadband laser with $\Delta\omega/\omega_0 = 1\%$ is

enhanced from 0.76×10^{15} to 1.12×10^{15} W/cm^2. Notably, the sunlight-like laser with $\Delta\omega/\omega_0 = 1\%$ can nearly double the SRS intensity threshold to 1.42×10^{15} W/cm^2. More importantly, the conventional broadband laser requires a nearly doubled bandwidth $\Delta\omega/\omega_0 = 2\%$ to reach an intensity threshold comparable to that of the sunlight-like laser with a bandwidth $\Delta\omega/\omega_0 = 1\%$. Further, the saturated reflectivity for the sunlight-like laser is also as low as that for the broadband laser with a doubled bandwidth. These results indicate that in contrast to the broadband laser, the sunlight-like laser significantly relaxes the bandwidth requirement for increasing the SRS intensity threshold and decreasing the saturated SRS reflectivity.

To compare the SRS reflectivities with different kinds of laser beams, it is important to make sure that the SRS develops into a quasi-steady state. In other words, the simulation time should be long enough that the SRS reflected light can reach saturation at least once. In the 1D PIC simulations, the total simulation time is set as $6000T_0$ (about 7 ps), which is long enough to achieve saturation of the SRS when the laser intensity is above the SRS threshold. The first saturation times of the SRS as functions of the laser intensity are compared for the three different laser types in Fig. 3(b). It is confirmed that the sunlight-like laser as well as the broadband laser can delay the saturation of the SRS, which is consistent with the results of a previous study.[42] It should be pointed out that when the laser intensity is below the SRS threshold, the corresponding SRS reflectivity will be nearly zero throughout the simulation, and hence the saturation time becomes meaningless and is not shown in Fig. 3(b).

In Fig. 3(c), the time evolutions of the electric fields of the backward-scattered light are displayed for three different kinds of laser beams. The laser intensity is set as $I = 3 \times 10^{15}$ W/cm^2, which is
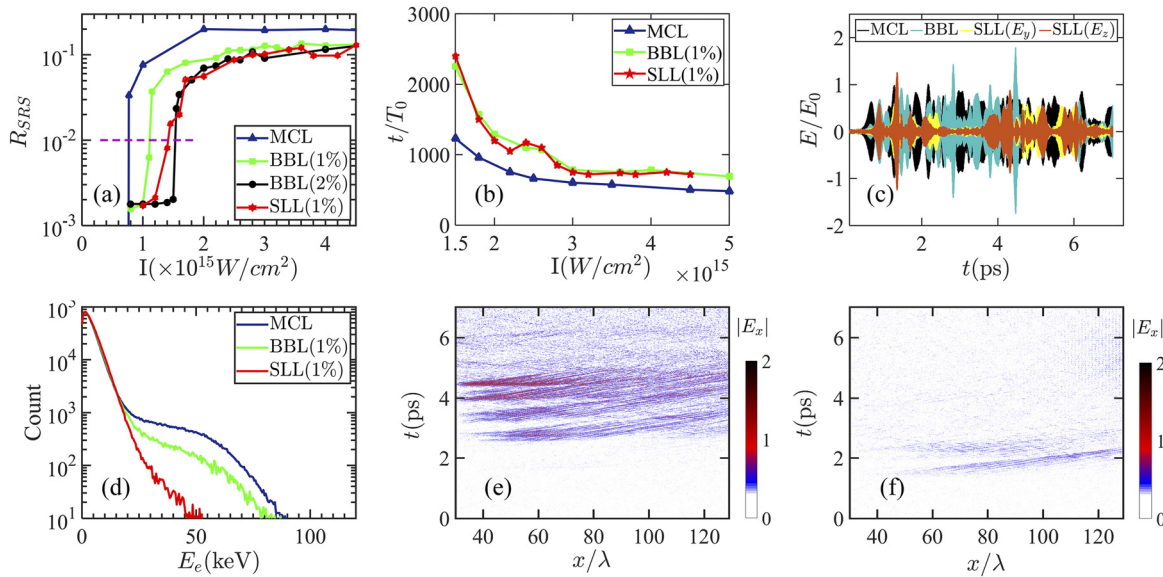

FIG. 3. (a) Average SRS reflectivity within $6000\lambda/c$ obtained from 1D PIC simulations as a function of laser intensity for a monochromatic laser (MCL), a broadband laser (BBL) with bandwidths $\Delta\omega/\omega_0 = 1\%$ and 2%, and a sunlight-like laser (SLL) with bandwidth $\Delta\omega/\omega_0 = 1\%$, respectively. The purple dashed line indicates $R_{SRS} = 1\%$. (b) First saturation time of the backward-reflected light as a function of laser intensity for the three different kinds of laser beams. (c) Time evolution of the electric field of the backward laser light, where all incident lasers have the same intensity of $I_0 = 3 \times 10^{15}$ W/cm^2, and both the broadband laser and sunlight-like laser have a bandwidth $\Delta\omega/\omega_0 = 1\%$. (d) Electron energy spectra for the monochromatic laser, broadband laser, and sunlight-like laser at the final simulation time of $6000\lambda/c$. (e) and (f) Time evolution of $|E_x|$ for the broadband laser and sunlight-like laser, respectively. In (b) and (d), all lasers have the same intensity $I_0 = 1.4 \times 10^{15}$ W/cm^2, and the broadband laser and sunlight-like laser have the same bandwidth $\Delta\omega/\omega_0 = 1\%$.

well above the threshold intensities for all three laser types to ensure that the SRS can fully develop into a quasi-steady state. Figure 3(c) also verifies that the sunlight-like laser as well as the broadband laser can delay the saturation of the SRS. Nevertheless, the first saturation of the SRS is reached before $t = 1000T_0$ in each case. Moreover, the scattered light behaves similarly after the quasi-steady state in all cases, i.e., bursting of the SRS reflectivity occurs. However, the SRS reflectivity R_{SRS} averaged within $t \leq 6000T_0$ is obviously different for the monochromatic ($R_{SRS} = 0.206$), broadband (0.172), and sunlight-like (0.107) lasers. From the point of view of the SRS reflectivity, one may conclude that the sunlight-like laser and the broadband laser are both effective in suppressing SRS.

The time evolution of the longitudinal electric field of E_x in Fig. 3(e) confirms that the SRS is excited by the broadband laser with $\Delta\omega/\omega_0 = 1\%$ at $I = 1.4 \times 10^{15}$ W/cm². By comparison, Fig. 3(f) verifies the efficient suppression of the SRS when the sunlight-like laser with the same bandwidth and intensity is used. Thanks to the efficient SRS suppression, hot-electron generation is gratifyingly reduced in the case of the sunlight-like laser, as evidenced in Fig. 3(d). Thus, the 1D PIC simulations indicate that the sunlight-like laser not only increases the intensity threshold of SRS, but also reduces the hot-electron generation in comparison with the broadband laser.

The superiority of sunlight-like lasers in mitigating parametric instabilities is further verified by 2D PIC simulations. In these simulations, the laser beams are assumed to propagate along the x direction, and the laser intensities are always uniform in the y direction. The polarization directions of the monochromatic laser and the broadband laser are both set to be along the z axis (i.e., there is S polarization). From the basic theory of SRS,[1] stimulated Raman sidescattering (SRSS) develops preferentially for S-polarized laser beams in a 2D geometry,[43,44] which is consistent with our simulations shown in Figs. 4(a) and 4(b). If the monochromatic laser and broadband laser are assumed to be polarized along the y axis (i.e., there is P polarization), our 2D simulations show that backward SRS will become the dominant instability, which is similar to the 1D simulation results and hence is not displayed here.

In Figs. 4(a)–4(c), we also plot the theoretical wavenumbers by numerically solving the equations for the three wave matching conditions and dispersion relations of each wave. In particular, the scattered light wave vector $\mathbf{k}_s$ in either Fig. 4(a) or Fig. 4(b) is nearly perpendicular to $\mathbf{k}_0$, i.e., SRSS develops predominantly. A comparison of the wavenumber intensity distributions for the monochromatic laser, broadband laser, and sunlight-like laser in Figs. 4(a)–4(c) clearly shows that a plasma wave due to SRS has been excited by the monochromatic laser or broadband laser at $1500T_0$, while it is greatly suppressed when the sunlight-like laser is used. These 2D PIC simulations indicate that the sunlight-like laser has a stronger suppressive effect on SRSS as well as on backward SRS. Consequently, as shown in Fig. 4(d), hot-electron generation is also dramatically reduced in the 2D case by using the sunlight-like laser.

IV. DISCUSSION AND CONCLUSION

Since SBS usually has a much smaller growth rate than SRS in a homogeneous plasma, the bandwidth required for suppression of SBS is usually much less than that for suppression of SRS.[26–28] In other words, SBS in a homogeneous plasma will usually be suppressed as long as SRS can be suppressed by using a broadband laser light. The above 1D and 2D simulations verify that a sunlight-like laser with a relatively low bandwidth is effective in mitigating SRS in a homogeneous plasma. Therefore, it is reasonable to infer that sunlight-like lasers will also perform well in mitigating other parametric instabilities such as SBS in the homogeneous plasmas relevant to indirect-drive ICF.

In the inhomogeneous plasmas relevant to direct-drive ICF, however, SRS may become convective, and the effect of laser bandwidth on the development of SRS will become more complex. Fluid-type simulations have shown that the enlargement of the SRS resonant region in the interactions of broadband lasers with inhomogeneous plasmas may increase the convective SRS gain,[45,46] even though broadband lasers decrease the SRS growth rate. Therefore, the net effect of broadband lasers on the development of SRS is not obvious in inhomogeneous plasmas. Recently, Wen et al.[47] studied the development of SRS in the interactions of broadband lasers with inhomogeneous plasmas in both the fluid and kinetic regimes. They found that the frequency modulation inherent in a broadband laser may compensate for the spatial detuning of SRS due to density inhomogeneity and hence enhance the SRS gain in an inhomogeneous plasma. A maximum-gain condition under which the SRS has its largest convective gain was derived in inhomogeneous plasmas, which indicates that the SRS convective gain will reach its peak value when the broadband frequency modulation effect cancels the spatial detuning due to density inhomogeneity.[47] Fortunately, the SRS
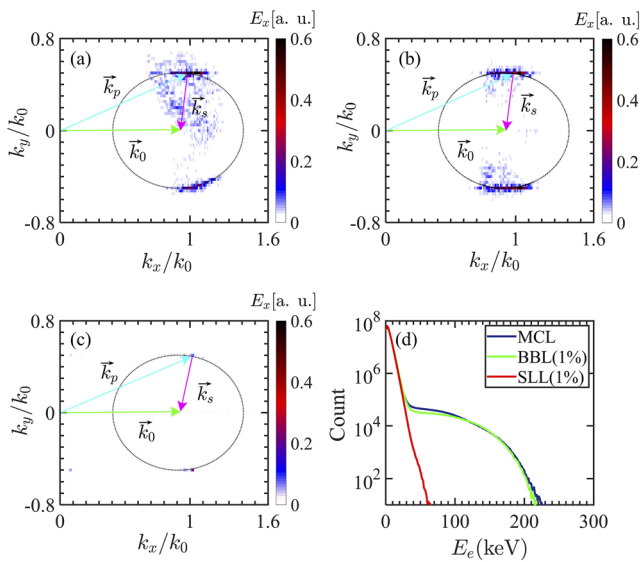
FIG. 4. Wave-vector distributions of the plasma wave field E_x at $1500T_0$ found from 2D PIC simulations for (a) a monochromatic laser (MCL), (b) a broadband laser (BBL), and (c) a sunlight-like laser (SLL). All possible plasma wave vectors are distributed around the theoretical dashed circles owing to the wave-vector and frequency matching conditions: $\mathbf{k}_0 = \mathbf{k}_s + \mathbf{k}_p$, $\omega_0 = \omega_s + \omega_p$, where the subscripts 0, s, and p refer to the incident, scattered, and plasma waves, respectively. (d) Corresponding electron energy spectra at the final time of $1500T_0$. All the lasers have the same intensity $I_0 = 1.4 \times 10^{15}$ W/cm², and the broadband laser and sunlight-like laser have the same bandwidth $\Delta\omega/\omega_0 = 1\%$. For simplicity, the laser intensity is assumed to be uniform in the y direction.

threshold could also be enhanced by tuning the parameters of the broadband laser far away from the maximum-gain condition.[47]

A sunlight-like laser beam comprises two orthogonally polarized broadband laser beams, and therefore the SRS gain may also be enhanced with a sunlight-like laser if the frequency modulation compensates for the spatial detuning of SRS in an inhomogeneous plasma. However, the random polarization of a sunlight-like laser itself will not broaden the resonant region of the SRS, but it will further increase the light incoherence and thus decrease the SRS growth rate. Therefore, a sunlight-like laser with random polarization is expected to have a better suppressive effect on SRS than a conventional broadband laser with the same bandwidth.

With the development of novel broad-bandwidth techniques,[29–31] broadband lasers with a bandwidth of one or a few percent have already been planned as next-generation ICF lasers. More importantly, numbers of driver laser beams are usually grouped into clusters to enter the hohlraum together. For example, 192 driver beams are grouped into 48 clusters of four beams in the NIF design.[4,7] Therefore, sunlight-like laser beams could be obtained in the beam clustering process as long as broadband laser beams are achieved, since Eq. (3) indicates that two broadband laser beams with orthogonal polarization states and independent random phase spectra can be combined to form a sunlight-like laser beam.

A sunlight-like laser beam can also be realized using only a single broadband laser beam with the help of polarization smoothing (PS). In this approach, an initial broadband laser beam is split by a wedged birefringent crystal into two orthogonally polarized broadband laser beams.[48] By using independent phase plates, different random phases can then be introduced into these two orthogonally polarized broadband laser beams. Finally, superposition of the two orthogonally polarized broadband beams can produce a sunlight-like laser beam.[34,49]

However, there are some differences between these two approaches to the realization of sunlight-like laser beams. In the first approach, broadband laser beams for the composition of a sunlight-like laser beam can be completely independent. For example, broadband laser beams before beam clustering can have different frequency spectra (e.g., flat-top or Gaussian) and different central frequencies. In the second approach, the two broadband laser beams obtained by PS always have the same frequency spectrum, since they come from the same initial broadband laser beam. Therefore, there may be more degrees of freedom available to decrease the light coherence in the first approach. On the other hand, PS can be further applied to a sunlight laser beam to reduce its spatial intensity inhomogeneity.

In summary, we have modeled a sunlight-like laser beam and proved its superiority in mitigating parametric instabilities in laser–plasma interactions for ICF research. To the best of our knowledge, this is the first precise model of a sunlight-like laser beam that has a given frequency spectrum, random phase spectrum, and random polarization state. We have found that compared with monochromatic lasers, the SRS intensity threshold can be nearly doubled using such a sunlight-like laser with a relatively low bandwidth $\Delta\omega/\omega_0 \simeq 1\%$, while a conventional broadband laser demands a doubled bandwidth $\Delta\omega/\omega_0 \simeq 2\%$ to achieve the same effect. Our 1D and 2D PIC simulations demonstrate that the plasma waves due to either backward or sideward SRS can be dramatically reduced by a sunlight-like laser with a relatively low bandwidth, and consequently the harmful hot-electron generation can be controlled well. It is expected that sunlight-like lasers will also be effective in suppressing other parametric instabilities in a similar manner owing to the degraded three-wave coupling in laser–plasma interactions. The next generation of ICF lasers could include sunlight-like laser drivers, realized as combinations of two or more broadband laser beams with independent phase spectra and orthogonal polarization states. This would be of great benefit in mitigating parametric instabilities in ICF.

SUPPLEMENTARY MATERIAL

See supplementary material for the detailed comparison between the different models of broadband laser lights. To visualize the random polarization state of a sunlight-like laser light, the time evolution of its electric field is also displayed in the supplementary movie.

ACKNOWLEDGMENTS

REFERENCES

[1]W. L. Kruer, *The Physics of Laser Plasma Interactions* (Addison-Wesley Publishing, 1988).

[2]C. S. Liu, *High-Power Laser-Plasma Interaction* (Cambridge University Press, 2019).

[3]T. R. Boehly, D. L. Brown, R. S. Craxton, R. L. Keck, J. P. Knauer, J. H. Kelly, T. J. Kessler, S. A. Kumpan, S. J. Loucks, S. A. Letzring, F. J. Marshall, R. L. McCrory, S. F. B. Morse, W. Seka, J. M. Soures, and C. P. Verdon, "Initial performance results of the OMEGA laser system," Opt. Commun. **133**, 495 (1997).

[4]C. A. Haynam, P. J. Wegner, J. M. Auerbach, M. W. Bowers, S. N. Dixit, G. V. Erbert, G. M. Heestand, M. A. Henesian, M. R. Hermann, K. S. Jancaitis, K. R. Manes, C. D. Marshall, N. C. Mehta, J. Menapace, E. Moses, J. R. Murray, M. C. Nostrand, C. D. Orth, R. Patterson, R. A. Sacks, M. J. Shaw, M. Spaeth, S. B. Sutton, W. H. Williams, C. C. Widmayer, R. K. White, S. T. Yang, and B. M. Van Wonterghem, "National Ignition Facility laser performance status," Appl. Opt. **46**, 3276 (2007).

[5]R. S. Craxton, K. S. Anderson, T. R. Boehly, V. N. Goncharov, D. R. Harding, J. P. Knauer, R. L. McCrory, P. W. McKenty, D. D. Meyerhofer, J. F. Myatt, A. J. Schmitt, J. D. Sethian, R. W. Short, S. Skupsky, W. Theobald, W. L. Kruer, K. Tanaka, R. Betti, T. J. B. Collins, J. A. Delettrez, S. X. Hu, J. A. Marozas, A. V. Maximov, D. T. Michel, P. B. Radha, S. P. Regan, T. C. Sangster, W. Seka, A. A. Solodov, J. M. Soures, C. Stoeckl, and J. D. Zuegel, "Direct-drive inertial confinement fusion: A review," Phys. Plasmas **22**, 110501 (2015).

[6]D. S. Montgomery, "Two decades of progress in understanding and control of laser plasma instabilities in indirect drive inertial fusion," Phys. Plasmas **23**, 055601 (2016).

[7]J. D. Lindl, P. Amendt, R. L. Berger, S. G. Glendinning, S. H. Glenzer, S. W. Haan, R. L. Kauffman, O. L. Landen, and L. J. Suter, "The physics basis for ignition using indirect-drive targets on the National Ignition Facility," Phys. Plasmas **11**, 339 (2004).

[8]R. Betti and O. A. Hurricane, "Inertial-confinement fusion with lasers," Nat. Phys. **12**, 435 (2016).

[9]J. C. Fernández, J. A. Cobble, B. H. Failor, D. F. DuBois, D. S. Montgomery, H. A. Rose, H. X. Vu, B. H. Wilde, M. D. Wilke, and R. E. Chrien, "Observed dependence of stimulated Raman scattering on ion-acoustic damping in hohlraum plasmas," Phys. Rev. Lett. **77**, 2702 (1996).

[10]P. Michel, L. Divol, E. L. Dewald, J. L. Milovich, M. Hohenberger, O. S. Jones, L. Berzak Hopkins, R. L. Berger, W. L. Kruer, and J. D. Moody, "Multibeam stimulated Raman scattering in inertial confinement fusion conditions," Phys. Rev. Lett. **115**, 055003 (2015).

[11]P. Neumayer, R. L. Berger, L. Divol, D. H. Froula, R. A. London, B. J. MacGowan, N. B. Meezan, J. S. Ross, C. Sorce, L. J. Suter, and S. H. Glenzer, "Suppression of stimulated Brillouin scattering by increased Landau damping in multiple-ion-species hohlraum plasmas," Phys. Rev. Lett. **100**, 105001 (2008).

[12]W. L. Kruer, S. C. Wilks, B. B. Afeyan, and R. K. Kirkwood, "Energy transfer between crossing laser beams," Phys. Plasmas **3**, 382 (1996).

[13]J. D. Moody, P. Michel, L. Divol, R. L. Berger, E. Bond, D. K. Bradley, D. A. Callahan, E. L. Dewald, S. Dixit, M. J. Edwards, S. Glenn, A. Hamza, C. Haynam, D. E. Hinkel, N. Izumi, O. Jones, J. D. Kilkenny, R. K. Kirkwood, J. L. Kline, W. L. Kruer, G. A. Kyrala, O. L. Landen, S. LePape, J. D. Lindl, B. J. MacGowan, N. B. Meezan, A. Nikroo, M. D. Rosen, M. B. Schneider, D. J. Strozzi, L. J. Suter, C. A. Thomas, R. P. J. Town, K. Widmann, E. A. Williams, L. J. Atherton, S. H. Glenzer, and E. I. Moses, "Multistep redirection by cross-beam power transfer of ultrahigh-power lasers in a plasma," Nat. Phys. **8**, 344 (2012).

[14]M. J. Rosenberg, A. A. Solodov, J. F. Myatt, W. Seka, P. Michel, M. Hohenberger, R. W. Short, R. Epstein, S. P. Regan, E. M. Campbell, T. Chapman, C. Goyon, J. E. Ralph, M. A. Barrios, J. D. Moody, and J. W. Bates, "Origins and scaling of hot-electron preheat in ignition-scale direct-drive inertial confinement fusion experiments," Phys. Rev. Lett. **120**, 055001 (2018).

[15]D. J. Strozzi, D. S. Bailey, P. Michel, L. Divol, S. M. Sepke, G. D. Kerbel, C. A. Thomas, J. E. Ralph, J. D. Moody, and M. B. Schneider, "Interplay of laser-plasma interactions and inertial fusion hydrodynamics," Phys. Rev. Lett. **118**, 025002 (2017).

[16]S. Skupsky, R. W. Short, T. Kessler, R. S. Craxton, S. Letzring, and J. M. Soures, "Improved laser-beam uniformity using the angular dispersion of frequency modulated light," J. Appl. Phys. **66**, 3456 (1989).

[17]S. N. Dixit, M. D. Feit, M. D. Perry, and H. T. Powell, "Designing fully continuous phase screens for tailoring focal-plane irradiance profiles," Opt. Lett. **21**, 1715–1717 (1996).

[18]D. H. Munro, S. N. Dixit, A. B. Langdon, and J. R. Murray, "Polarization smoothing in a convergent beam," Appl. Opt. **43**, 6639 (2004).

[19]J. Fuchs, C. Labaune, S. Depierreux, H. A. Baldis, and A. Michard, "Modification of spatial and temporal gains of stimulated Brillouin and Raman scattering by polarization smoothing," Phys. Rev. Lett. **84**, 3089 (2000).

[20]Ph. Mounaix, L. Divol, S. Hüller, and V. T. Tikhonchuk, "Effects of spatial and temporal smoothing on stimulated Brillouin scattering in the independent-hot-spot model limit," Phys. Rev. Lett **85**, 4526 (2000).

[21]J. D. Moody, B. J. MacGowan, J. E. Rothenberg, R. L. Berger, L. Divol, S. H. Glenzer, R. K. Kirkwood, E. A. Williams, and P. E. Young, "Backscatter reduction using combined spatial, temporal, and polarization beam smoothing in a long-scale-length laser plasma," Phys. Rev. Lett. **86**, 2810 (2001).

[22]D. H. Froula, L. Divol, R. L. Berger, R. A. London, N. B. Meezan, D. J. Strozzi, P. Neumayer, J. S. Ross, S. Stagnitto, L. J. Suter, and S. H. Glenzer, "Direct measurements of an increased threshold for stimulated Brillouin scattering with polarization smoothing in ignition hohlraum plasmas," Phys. Rev. Lett. **101**, 115002 (2008).

[23]B. J. Winjum, F. S. Tsung, and W. B. Mori, "Mitigation of stimulated Raman scattering in the kinetic regime by external magnetic fields," Phys. Rev. E **98**, 043208 (2018).

[24]B. J. Albright, L. Yin, and B. Afeyan, "Control of stimulated Raman scattering in the strongly nonlinear and kinetic regime using spike trains of uneven duration and delay," Phys. Rev. Lett. **113**, 045002 (2014).

[25]I. Barth and N. J. Fisch, "Reducing parametric backscattering by polarization rotation," Phys. Plasmas **23**, 102106 (2016).

[26]W. L. Kruer, K. G. Estabook, and K. H. Sinz, "Instability generated laser reflection in plasmas," Nucl. Fusion **13**, 952 (1973).

[27]J. J. Thomson and J. I. Karush, "Effects of finite-bandwidth driver on the parametric instability," Phys. Fluids **17**, 1608 (1974).

[28]S. P. Obenschain, N. C. Luhmann, and P. T. Greiling, "Effects of finite-bandwidth driver pumps on the parametric-decay instability," Phys. Rev. Lett. **36**, 1309 (1976).

[29]J. Weaver, R. Lehmberg, S. Obenschain, D. Kehne, and M. Wolford, "Spectral and far-field broadening due to stimulated rotational Raman scattering driven by the Nike krypton fluoride laser," Appl. Opt. **56**, 8618 (2017).

[30]Y. Cui, Y. Gao, D. Rao, D. Liu, F. Li, L. Ji, H. Shi, J. Liu, X. Zhao, W. Feng, L. Xia, J. Liu, X. Li, T. Wang, W. Ma, and Z. Sui, "High-energy low-temporal-coherence instantaneous broadband pulse system," Opt. Lett. **44**, 2859 (2019).

[31]C. Dorrer, E. M. Hill, and J. D. Zuegel, "High-energy parametric amplification of spectrally incoherent broadband pulses," Opt. Express **28**, 451–471 (2020).

[32]J. E. Santos, L. O. Silva, and R. Bingham, "White light parametric instabilities in plasmas," Phys. Rev. Lett. **98**, 235001 (2007).

[33]Y. Zhao, S. M. Weng, M. Chen, J. Zheng, H. B. Zhuo, C. Ren, Z. M. Sheng, and J. Zhang, "Effective suppression of parametric instabilities with decoupled broadband lasers in plasma," Phys. Plasmas **24**, 112102 (2017).

[34]R. K. Follett, J. G. Shaw, J. F. Myatt, J. P. Palastro, R. W. Short, and D. H. Froula, "Suppressing two-plasmon decay with laser frequency detuning," Phys. Rev. Lett. **120**, 135005 (2018).

[35]J. A. Marozas, M. Hohenberger, M. J. Rosenberg, D. Turnbull, T. J. B. Collins, P. B. Radha, P. W. McKenty, J. D. Zuegel, F. J. Marshall, S. P. Regan, T. C. Sangster, W. Seka, E. M. Campbell, V. N. Goncharov, M. W. Bowers, J.-M. G. Di Nicola, G. Erbert, B. J. MacGowan, L. J. Pelz, and S. T. Yang, "First observation of cross-beam energy transfer mitigation for direct-drive inertial confinement fusion implosions using wavelength detuning at the National Ignition Facility," Phys. Rev. Lett. **120**, 085001 (2018).

[36]J. W. Bates, J. F. Myatt, J. G. Shaw, R. K. Follett, J. L. Weaver, R. H. Lehmberg, and S. P. Obenschain, "Mitigation of cross-beam energy transfer in inertial-confinement-fusion plasmas with enhanced laser bandwidth," Phys. Rev. E **97**, 061202 (2018).

[37]R. K. Follett, J. G. Shaw, J. F. Myatt, C. Dorrer, D. H. Froula, and J. P. Palastro, "Thresholds of absolute instabilities driven by a broadband laser," Phys. Plasmas **26**, 062111 (2019).

[38]J. Tinbergen, *Astronomical Polarimetry* (Cambridge University Press, 1996).

[39]T. D. Arber, K. Bennett, C. S. Brady, A. Lawrence-Douglas, M. G. Ramsay, N. J. Sircombe, P. Gillies, R. G. Evans, H. Schmitz, A. R. Bell, and C. P. Ridgers, "Contemporary particle-in-cell approach to laser-plasma modelling," Plasma Phys. Controlled Fusion **57**, 113001 (2015).

[40]D. S. Montgomery, J. A. Cobble, J. C. Fernández, R. J. Focia, R. P. Johnson, N. Renard-LeGalloudec, H. A. Rose, and D. A. Russell, "Recent trident single hot spot experiments: Evidence for kinetic effects, and observation of Langmuir decay instability cascade," Phys. Plasmas **9**, 2311 (2002).

[41]L. Yin, W. Daughton, B. J. Albright, B. Bezzerides, D. F. DuBois, J. M. Kindel, and H. X. Vu, "Nonlinear development of stimulated Raman scattering from electro-static modes excited by self-consistent non-Maxwellian velocity distributions," Phys. Rev. E **73**, 025401 (2006).

[42]Y. Zhao, L.-L. Yu, J. Zheng, S.-M. Weng, C. Ren, C.-S. Liu, and Z.-M. Sheng, "Effects of large laser bandwidth on stimulated Raman scattering instability in underdense plasma," Phys. Plasmas **22**, 052119 (2015).

[43]K. Q. Pan, S. E. Jiang, Q. Wang, L. Guo, S. W. Li, Z. C. Li, D. Yang, C. Y. Zheng, B. H. Zhang, and X. T. He, "Two-plasmon decay instability of the backscattered light of stimulated Raman scattering," Nucl. Fusion **58**, 096035 (2018).

[44]H. Wen, A. V. Maximov, R. Yan, J. Li, C. Ren, and F. S. Tsung, "Three-dimensional particle-in-cell modeling of parametric instabilities near the quarter-critical density in plasmas," Phys. Rev. E **100**, 041201 (2019).

[45]P. N. Guzdar, C. S. Liu, and R. H. Lehmberg, "The effect of bandwidth on the convective Raman instability in inhomogeneous plasmas," Phys. Fluids B **3**, 2882 (1991).

[46]P. N. Guzdar, C. S. Liu, and R. H. Lehmberg, "Induced spatial incoherence effects on the convective Raman instability," Phys. Fluids B **5**, 910 (1993).

[47]H. Wen, R. K. Follett, A. V. Maximov, D. H. Froula, F. S. Tsung, and J. P. Palastro, "Suppressing the enhancement of stimulated Raman scattering in inhomogeneous plasmas by tuning the modulation frequency of a broadband laser," Phys. Plasmas **28**, 042109 (2021).

[48]T. R. Boehly, V. A. Smalyuk, D. D. Meyerhofer, J. P. Knauer, D. K. Bradley, R. S. Craxton, M. J. Guardalben, S. Skupsky, and T. J. Kessler, "Reduction of laser imprinting using polarization smoothing on a solid-state fusion laser," J. Appl. Phys. **85**, 3444 (1999).

[49]R. K. Follett, J. G. Shaw, J. F. Myatt, H. Wen, D. H. Froula, and J. P. Palastro, "Thresholds of absolute two-plasmondecay and stimulated Raman scattering instabilities driven by multiple broadband lasers," Phys. Plasmas **28**, 032103 (2021).